

## Research Paper

### Analysis of Estimation of Parameters in 3P-Weibull $K_{Jc}$ Distribution: Sample Size Effect

Diego Omar ALIAS<sup>1)</sup>, Juan Elías PEREZ IPIÑA<sup>2)</sup>, Carlos BEREJNOI<sup>3)</sup>\*

<sup>1)</sup> *Comisión Nacional de Energía Atómica  
Instituto Sábato, Universidad Nacional de San Martín*

Argentina  
e-mail: diegoalias@hotmail.com

<sup>2)</sup> *COPPE-UFRJ Rio de Janeiro, Brasil  
CONICET, Neuquén, Argentina*

e-mail: pipinajuan@gmail.com

<sup>3)</sup> *Facultad de Ingeniería  
Consejo de Investigación de la Universidad Nacional de Salta – CIUNSa  
Universidad Nacional de Salta*

Argentina

\*Corresponding Author e-mail: berejnoi@gmail.com

The minimum sample size for a good estimation of the parameters in both three-parameter Weibull  $K_{Jc}$  distribution (3P-W) and ASTM E1921 methods was analyzed. Additionally, the estimations provided by maximum likelihood (ML) and linear regression (LR) were compared. Fracture toughness sets with different sample sizes were randomly generated following a 3P-W with parameters corresponding to experimental datasets from the Euro round robin fracture toughness test. Then, LR and ML were applied to the sets and the parameters were estimated. Standard deviation (SD) and interquartile range (IQR) were employed to analyze the goodness of fit. The results of this paper were consistent with the necessity of large sample sizes (over 30) to find a representative value of the threshold and shape parameters. However, the scale parameter showed a lower scatter and can be estimated with a smaller sample size (around six samples), as used in the standard ASTM E1921-19<sup>p</sup>.

**Key words:** ductile-to-brittle transition; three-parameter Weibull distribution; convergence of estimated values.

#### NOTATIONS

- $b$  – shape parameter of a three-parameter Weibull,
- $f(K_{Jc})$  – density probability function of a three-parameter Weibull distribution,
- $F(K_{Jc})$  – cumulative function of a three-parameter Weibull distribution,

$F_i$	–	cumulative probability that corresponds to the $i$ -th value in a set of data,
IQR	–	interquartile range,
$J_c$	–	experimental $J$ -integral at the onset of cleavage fracture,
$K_{Jc}$	–	critical $K$ value converted from $J_c$ ,
$K_{Jci}$	–	the $i$ -th $K_{Jc}$ value in a set of data,
$K_{Jcmed}$	–	median $K_{Jc}$ in a set of data,
$K_{min}$	–	threshold parameter of a three-parameter Weibull distribution,
$K_0$	–	scale parameter of a three-parameter Weibull distribution,
$L$	–	likelihood function,
LR	–	linear regression method,
Master Curve	–	transition curve defined in the ASTM E1921 standard,
ML	–	maximum likelihood method,
$n$	–	number of specimens in a set of toughness values,
$P_i$	–	percentile estimator,
$Q_1$	–	first quartile,
$Q_3$	–	third quartile,
$R^2$	–	coefficient of determination,
SD	–	standard deviation,
$T_0$	–	reference temperature defined in the ASTM E1921 standard,
$X$	–	parameter value ( $K_{min}$ , $K_0$ , $b$ ),
$X_i$	–	estimator value,
$\bar{X}$	–	$X_i$ mean,
3P-W	–	three-parameter Weibull distribution.

## 1. INTRODUCTION

The fracture mechanics study of structural steel behavior in the ductile-to-brittle transition has been the subject of many research papers during the last 50 years. Different fracture mechanics-based criteria can be used in order to determine fracture toughness for crack instability, even for relatively large amounts of crack-tip plasticity and previous-to-fracture stable crack growth. The most used criterion is  $J_c$ , which is usually converted to  $K_{Jc}$  equivalent.

In 1980, LANDES and SHAFFER [1] observed a large scatter of fracture toughness test results, for a given temperature, related to a specimen size effect, and proposed a two-parameter Weibull distribution to fit the dispersion in experimental  $J_c$  values. In 1984, LANDES and MCCABE [2] added a third parameter to the Weibull distribution – the threshold parameter – because the fracture toughness value predicted by the weakest link model based on a two-parameter Weibull distribution tendency toward zero as the specimen size becomes very large. Additionally, WALLIN *et al.* [3] proposed the Wallin, Saario, Törrönen (WST) model, which also uses a three-parameter Weibull (3P-W) distribution in terms of  $K$  with two of them fixed, and relates the macro-behavior with micromechanisms [3, 4].

This combination of scatter and specimen size effect at a given temperature makes it complex and expensive to obtain the experimental behavior in the whole transition region. Moreover, there are limitations, given by extensive plasticity and large stable crack growth at the superior third of the transition, that make it practically impossible to have a valid sample for specimen sizes normally tested in the laboratory.

WALLIN proposed [5] that the medium toughness values for a one-inch thickness follow a unique curve – the master curve – regardless of the ferritic steel grade, and the value of the reference temperature  $T_0$  is only needed to position it on the temperature axis.  $T_0$  is the temperature at which  $K_{Jc\text{ med}}$  is  $100 \text{ MPa} \cdot \sqrt{\text{m}}$ , for a thickness of one inch. Once  $T_0$  is obtained, the fracture toughness distribution, consisting in a 3P-W with two of its parameters pre-defined as constant, can be estimated for different temperatures and sizes [6, 7]. Determining  $T_0$  to calibrate the master curve is specified by ASTM E1921 test method that was standardized in 1997 and, since then, improved several times [8]. Six valid tests are sufficient to estimate  $T_0$ . Recent studies about this subject account for the  $T_0$  estimation based on precracked Charpy and non-standard specimens [9–11], constraint effects [12–15], and alternatives to the master curve for lower bound estimations [16, 17]. The goodness of  $T_0$  estimation for different temperatures and sizes was also studied [18, 19]. The estimation of  $T_0$  is performed with  $K_{Jc}$  values, i.e., values of  $J_c$  converted to  $K$ -equivalent. More recently, it was shown that a 3P-W expressed in terms of  $J$  could not be converted into an equivalent 3P-W in  $K$  [20].

### 1.1. The 3P-W distribution

The 3P-W distribution, proposed by WEIBULL [21] in 1951, has a probability density function  $f(K_{Jc})$  and a cumulative distribution function  $F(K_{Jc})$  as Eqs (1.1) and (1.2) show respectively:

$$(1.1) \quad f(K_{Jc}; K_{\min}, K_0, b) = \frac{b}{K_0 - K_{\min}} \left( \frac{K_{Jc} - K_{\min}}{K_0 - K_{\min}} \right)^{b-1} \exp \left[ - \left( \frac{K_{Jc} - K_{\min}}{K_0 - K_{\min}} \right)^b \right],$$

$$(1.2) \quad F(K_{Jc}) = 1 - \exp \left[ - \left( \frac{K_{Jc} - K_{\min}}{K_0 - K_{\min}} \right)^b \right],$$

where  $K_{\min}$  – threshold parameter,  $K_0$  – scale parameter,  $b$  – shape parameter.

The methods used for estimating all the three parameters of 3P-W can be graphical or analytical [22]. The most commonly used graphical method is based on the Weibull plot [22]. LR and ML are analytical methods, the latter one being the most widely used because it provides efficient estimators (asymptotically normally distributed and asymptotically unbiased [23, 24]). However, as

this method does not have a closed-form solution, numerical methods must be applied. LR and ML are briefly presented in Sec. 2.

Based on limitations related to costs and material availability, especially in irradiated material in the nuclear industry, it is important to test the least number of specimens necessary to have a good estimation of the statistical parameters. In this way, the main objective of this paper was to analyze the minimum sample size ( $n$ ) that provides a good estimation of each of the parameters in both 3P-W (estimating the three parameters) and ASTM E1921 (estimating only  $K_0$ , with  $K_{\min}$  and  $b$  being fixed) methods. Additionally, the estimations provided by ML and LR, the latter using four percentile estimators, were also compared.

## 2. MATERIALS AND METHODS

### 2.1. Method of Linear Regression (LR)

Using algebraic manipulation over Eq. (1.2):

$$(2.1) \quad \ln \ln \frac{1}{1-F} = b \ln (K_{Jc} - K_{\min}) - b \ln (K_0 - K_{\min}).$$

The use of logarithm drives to a linear relationship, where the slope is the parameter  $b$ , making it possible to calculate the  $K_0$  parameter from the last term of the second member in Eq. (2.1).  $K_{Jci}$  is the  $i$ -th  $K_{Jc}$  value in the sample, and  $F_i$  is its probability based on the percentile estimator used [24]. The square minimum is used to find the line that best fits the sample, and the coefficient of determination  $R^2$  refers to the fit quality.

### 2.2. Method of Maximum Likelihood (ML)

In this analytical method, the estimated parameters are those which make the likelihood function (Eq. (2.2)) a maximum. As the closed-form solution is not possible to be obtained, the Newton-Raphson method is usually applied.

$$(2.2) \quad L(K_{\min}, K_0, b) = \prod_{i=1}^n (K_{Jci}, K_{\min}, K_0, b).$$

### 2.3. Data generation

Datasets of around 30 tests each, taken from experimental results corresponding to the Euro round robin fracture toughness test [25], were used in this paper. 3P-W distribution parameters were estimated by using ML. Then, artificial sets of different sizes were generated from each of the selected datasets to perform the analyses.

Table 1 presents the selected datasets, including the estimated parameters. The quantity of censored values, according to the criterion stated in ASTM E1921 standard, is also included in the Table. Only datasets with a minimum number of censored values were chosen for generating simulated new sets to avoid perturbations in the estimations of 3P-W parameters. Using the estimated parameters from Table 1, sets of different sizes ( $n = 5, 6, 8, 10, 20, 30, 40, 50, 60$ ) were generated by applying the Monte Carlo method, based on Donald E. Knuth's subtractive random number generator algorithm [26]. In order to get a repeatable simulation, 3000 sets were generated for each size ( $n$ ) and dataset.

LR and ML were employed to estimate the parameters from the generated sets.

**Table 1.** Datasets of values used for data generation.

Dataset	$T$ [°C]	Thickness [mm]	Experimental dataset size	Censored	$K_{\min}$ [MPa·√m]	$K_0$ [MPa·√m]	$b$
# 1	-154	50.00	30	0	29.46	37.78	1.35
# 2	-110	12.50	55	0	33.42	87.65	3.00
# 3	-91	12.50	31	0	45.22	121.88	2.99
# 4	-60	12.50	31	2	80.63	159.47	2.04
# 5	-20	100.00	15	0	129.96	208.18	3.57

The percentile estimators used in the LR method are shown in Eqs (2.3) to (2.6).

$$(2.3) \quad P_i = \frac{i - 0.3}{n + 0.4},$$

$$(2.4) \quad P_i = \frac{i - 0.5}{n},$$

$$(2.5) \quad P_i = \frac{i - 3/8}{n + 1/4},$$

$$(2.6) \quad P_i = \frac{i}{n + 1}.$$

#### 2.4. Analysis of scatter

IQR [27] and SD were employed to quantitatively compare the scatter of the estimated parameter values with a different number of samples. They were normalized over the parameter that generated the simulated sets (Eqs (2.7) and (2.8)) and plotted versus the sample size  $n$ :

$$(2.7) \quad \frac{\text{IQR}}{X} = \frac{Q_3 - Q_1}{X},$$

$$(2.8) \quad \frac{\text{SD}}{X} = \frac{\sqrt{\frac{1}{3000-1} \sum_{i=1}^{3000} (X_i - \bar{X})^2}}{X},$$

where  $X$  is the value of the generator parameter ( $K_{\min}; K_0; b$ ),  $X_i$  is the estimator value,  $\bar{X}$  is estimator sample mean, 3000 corresponds to the number of sets generated,  $Q_1$  is the first interquartile, and  $Q_3$  is the third interquartile.

Figure 1 shows the procedure for the calculation of  $\text{IQR}/X$  and  $\text{SD}/X$  values for each sample size  $n$ .

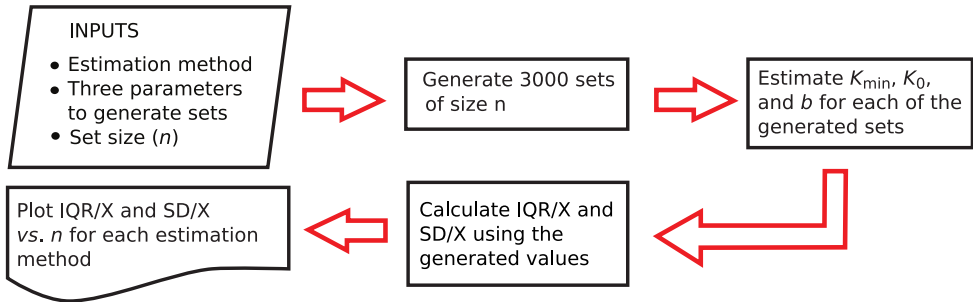


FIG. 1. Procedure employed in the analysis of scatter.

Boxplots (see Fig. 2) were included to show the scatter presented by each estimated parameter. In this case, the box itself shows the IQR, and the line

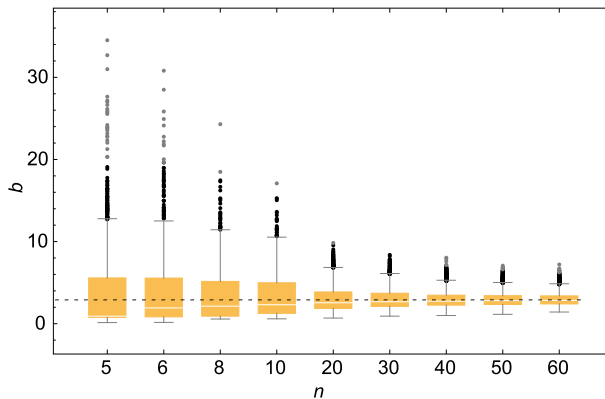


FIG. 2. Boxplot for  $b$ , using the ML method. Parameters used in the generation process:  $K_{\min} = 33.42 \text{ MPa} \cdot \sqrt{\text{m}}$ ,  $K_0 = 87.65 \text{ MPa} \cdot \sqrt{\text{m}}$  and  $b = 3$ , corresponding to dataset No. 2.

inside the box represents the median. Besides, the whiskers correspond to values that are 1.5 IQR above or below the 3rd and 1st interquartiles, respectively; the outliers are indicated by black dots and the far outliers by grey dots [23]. The parameter value used for data generation is indicated as a dashed line.

### 3. RESULTS

Figures 2 to 4 show examples of boxplots corresponding to the 3000 estimations for each set size of the three parameters, i.e.,  $K_0$ ,  $b$ , and  $K_{\min}$ . As the five estimations obtained in each case (four by means of LR and one with ML)

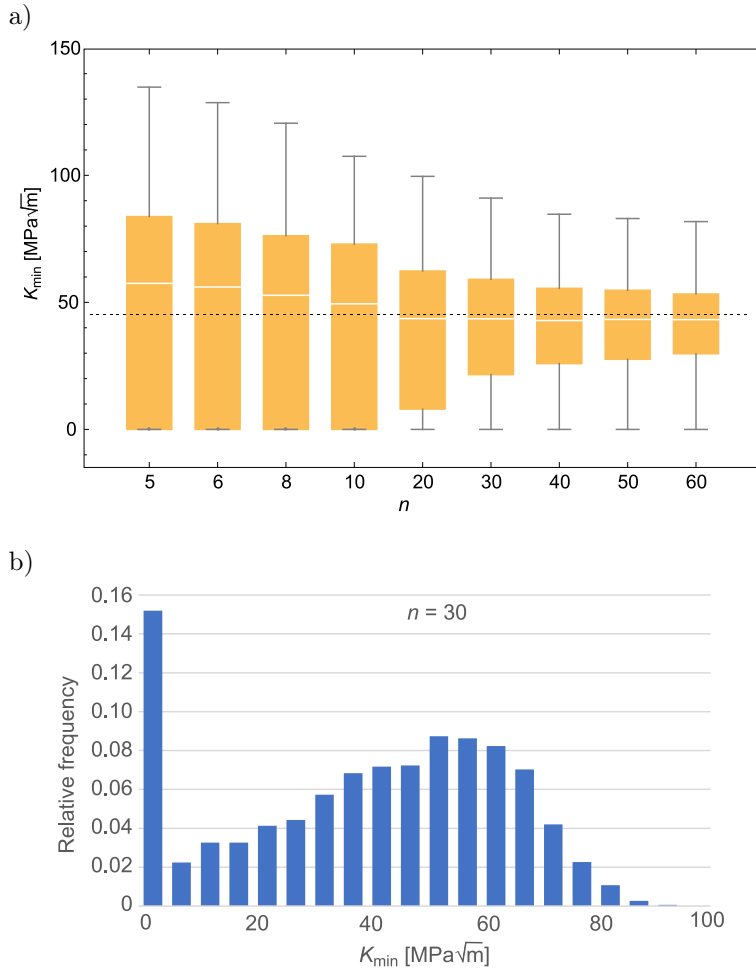


FIG. 3. a) Boxplot for  $K_{\min}$ , LR method, percentile estimator 1, Eq. (2.3); b) histogram for  $K_{\min}$  with  $n = 30$ . Parameters used in the generation process:  $K_{\min} = 45.22 \text{ MPa}\cdot\sqrt{\text{m}}$ ,  $K_0 = 121.88 \text{ MPa}\cdot\sqrt{\text{m}}$  and  $b = 2.99$ , corresponding to dataset No. 3.

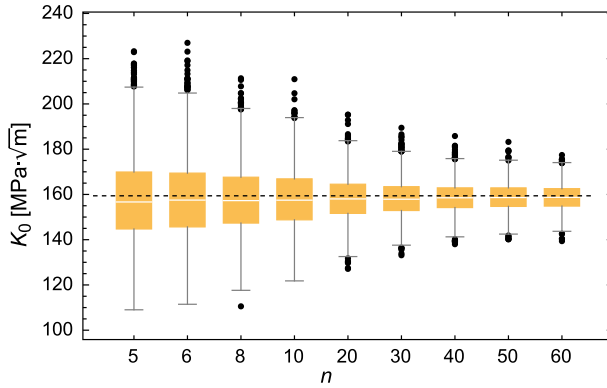


FIG. 4. Boxplot for  $K_0$  estimations, using ML method. Parameters used in the generation process:  $K_{\min} = 80.63 \text{ MPa} \cdot \sqrt{\text{m}}$ ,  $K_0 = 159.47 \text{ MPa} \cdot \sqrt{\text{m}}$ , and  $b = 2.04$ , corresponding to dataset No. 4.

presented similar convergences, only one case is shown. Figure 3b shows the histogram of  $K_{\min}$  estimations when  $n = 30$  and  $b > 2$ .

Figures 5 to 7 and 8 to 10 show examples of the plots of  $\text{IQR}/X$  and  $\text{SD}/X$  for the three Weibull parameters, respectively. The points identified by means of Est1, Est2, Est3 and Est4 in the figures correspond to the use of Eqs. (2.3) to (2.6) for estimating the percentiles that generate the estimated parameters used to calculate  $\text{IQR}/X$  and  $\text{SD}/X$  values. In the case of ASTM E1921 standard, this analysis was performed only to estimate  $K_0$  by ML, with the other parameters fixed ( $K_{\min} = 20 \text{ MPa} \cdot \sqrt{\text{m}}$  and  $b = 4$ ).

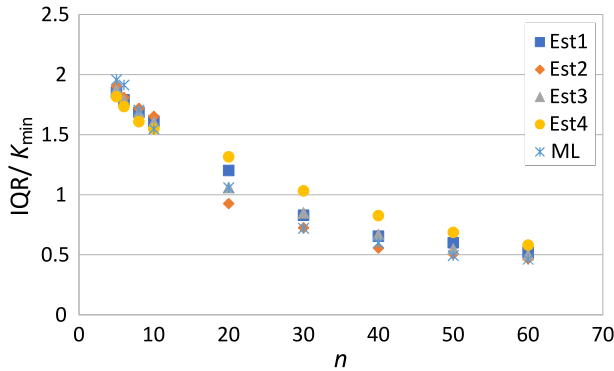


FIG. 5.  $\text{IQR}/K_{\min}$  versus set size  $n$ . Values generated using  $K_{\min} = 45.22 \text{ MPa} \cdot \sqrt{\text{m}}$ ,  $K_0 = 121.88 \text{ MPa} \cdot \sqrt{\text{m}}$  and  $b = 2.99$  (dataset No. 3).

Table 2 shows one example of  $\text{IQR}/X$  and  $\text{SD}/X$  values, for  $n = 6$  and  $n = 20$ , and the ratio between these values expressed as  $\text{IQR}_{20}/\text{IQR}_6$  and  $\text{SD}_{20}/\text{SD}_6$ .

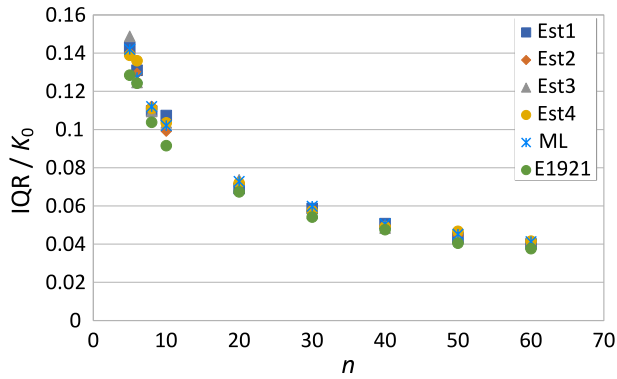


FIG. 6.  $IQR/K_0$  versus set size  $n$ , including  $K_0$  values estimated by ASTM E1921. Values generated using  $K_{\min} = 45.22 \text{ MPa} \cdot \sqrt{\text{m}}$ ,  $K_0 = 121.88 \text{ MPa} \cdot \sqrt{\text{m}}$  and  $b = 2.99$  (dataset No. 3).

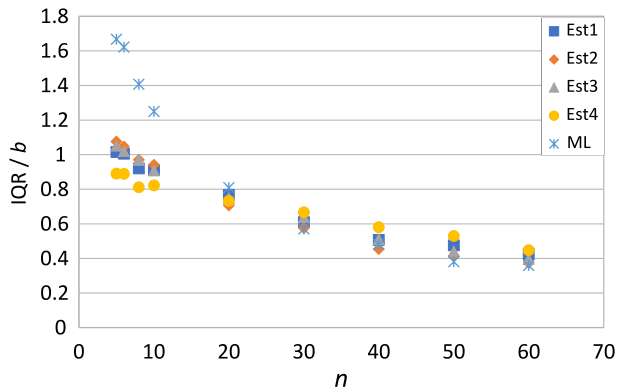


FIG. 7.  $IQR/b$  versus set size  $n$ . Values generated using  $K_{\min} = 45.22 \text{ MPa} \cdot \sqrt{\text{m}}$ ,  $K_0 = 121.88 \text{ MPa} \cdot \sqrt{\text{m}}$  and  $b = 2.99$  (dataset No. 3).

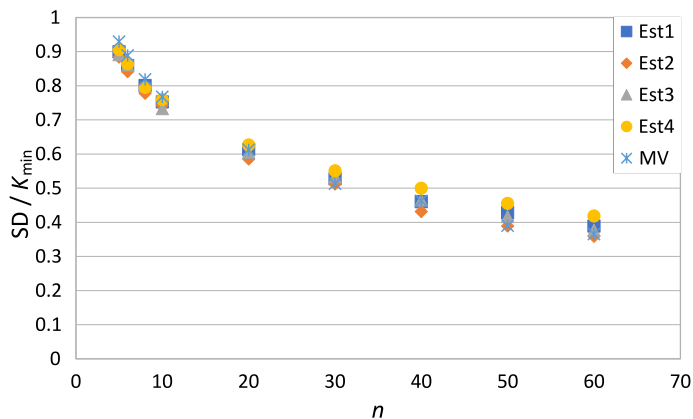


FIG. 8.  $SD/K_{\min}$  versus set size  $n$ . Values generated using  $K_{\min} = 45.22 \text{ MPa} \cdot \sqrt{\text{m}}$ ,  $K_0 = 121.88 \text{ MPa} \cdot \sqrt{\text{m}}$  and  $b = 2.99$  (dataset No. 3).

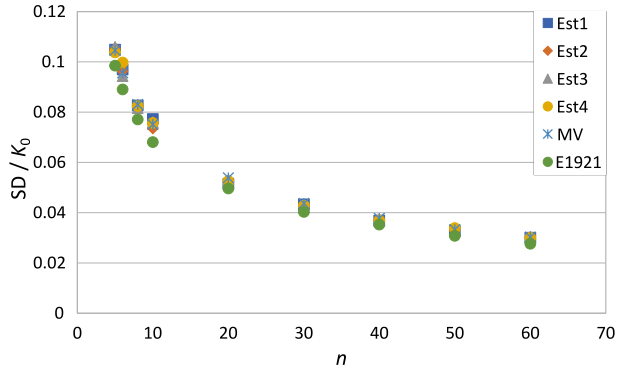


FIG. 9.  $SD/K_0$  versus set size  $n$ , including  $K_0$  values estimated by ASTM E1921. Values generated using  $K_{\min} = 45.22 \text{ MPa} \cdot \sqrt{\text{m}}$ ,  $K_0 = 121.88 \text{ MPa} \cdot \sqrt{\text{m}}$  and  $b = 2.99$  (dataset No. 3).

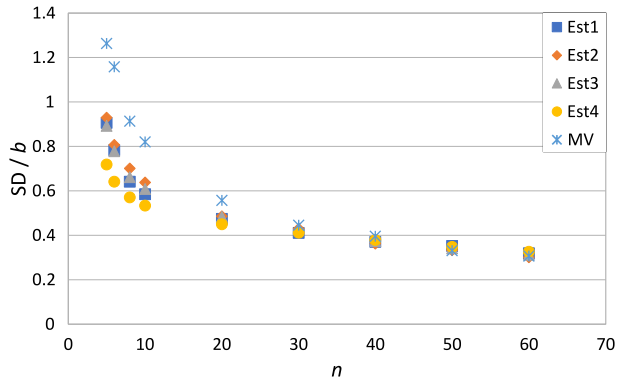


FIG. 10.  $SD/b$  versus set size  $n$ . Values generated using  $K_{\min} = 45.22 \text{ MPa} \cdot \sqrt{\text{m}}$ ,  $K_0 = 121.88 \text{ MPa} \cdot \sqrt{\text{m}}$ ,  $b = 2.99$  (dataset No. 3).

**Table 2.**  $IQR/X$  and  $SD/X$  ratios between  $n = 6$  and  $n = 20$ , dataset No. 3.

		$n = 6$	$n = 20$	$IQR_{20}/IQR_6$			$n = 6$	$n = 20$	$SD_{20}/SD_6$
$IQR/K_{\min}$	LR	1.78	1.126	0.63	$SD/K_{\min}$	LR	0.857	0.608	0.71
	ML	1.913	1.058	0.55		ML	0.889	0.613	0.69
$IQR/K_0$	LR	0.13	0.072	0.55	$SD/K_0$	LR	0.097	0.052	0.54
	ML	0.127	0.073	0.57		ML	0.096	0.054	0.56
	E1921	0.124	0.067	0.54		E1921	0.089	0.05	0.56
$IQR/b$	LR	0.99	0.738	0.75	$SD/b$	LR	0.753	0.473	0.63
	ML	1.621	0.809	0.50		ML	1.159	0.557	0.48

## 4. DISCUSSION

Well-known datasets were analyzed in order to study the reliability of the 3P-W estimation of parameters from a statistical point of view. Although ASTM E1921 allows the use of censoring, and different alternatives were proposed in the literature [28, 29]. Nevertheless, no censoring was applied in this work to avoid perturbations in the results by non-valid tests according to ASTM E1921. This subject, censoring, is part of new research under development. In this paper, five datasets were selected with few or no censored results. As the datasets are around 30 specimens each, it was assumed that any method would give an acceptable estimation of the three Weibull parameters, so ML was employed. Three thousand sets for each  $n$  and each dataset were generated using the Monte Carlo method. Then, ML and LR (with 4 different estimators) were used to estimate the 3P-W parameters, and were contrasted and compared. A total number of 3000 sets were selected to ensure enough repeatability. The three methods of analysis of goodness of fit were selected for different reasons:

- a) Boxplots as they expose the scatter intuitively and provide a good tool to compare the scatter visually as a function of the set sizes;
- b) IQR as it is also an intuitive way to measure the scatter but is not significantly affected by asymmetric distributions as the ones observed in the transition range [30]; and
- c) SD is applied because most of the analysis in transition results uses this indicator as a measure of scatter, although it is not insensitive to asymmetry.

All the figures from 2 to 10 (as well as all not shown results) depict that, as expected, scatter decreases as sample size increases. IQR/ $X$  greatly decreases between  $n = 6$  and  $n = 20$ . For  $n = 20$  and over, the values of IQR/ $X$  do not show a considerable change of slope. SD/ $X$  values follow the same tendency.

SD did not produce qualitative differences between the estimation methods for the  $K_{\min}$  and  $K_0$  estimated values (Figs 8 and 9). Instead, there were differences for the parameter  $b$ , the lowest SD corresponding to the estimator number 4 in LR ( $P_i = \frac{i}{n+1}$ ), while the highest corresponding to ML (Fig. 10). This pattern was observed in all the datasets, except for dataset No. 1. According to WALLIN [31], the test temperature of this dataset ( $-154^\circ\text{C}$ ) corresponds to the lower shelf region of fracture toughness.

When comparing scatter values between the three parameters, large differences were observed, independently of the estimation method, the set and the evaluation method (IQR, SD).  $K_0$  produced scatters that were at least one order of magnitude lower than the other two parameters  $K_{\min}$  and  $b$ , and a faster convergence with the number of tests.

Table 2 shows that the estimated  $K_{\min}$  values presented a large scatter for  $n = 6$ , i.e., for  $K_{\min} = 40 \text{ MPa} \cdot \sqrt{\text{m}}$ , being the corresponding IQR between  $71 \text{ MPa} \cdot \sqrt{\text{m}}$  and  $77 \text{ MPa} \cdot \sqrt{\text{m}}$ , depending on whether LR or ML is used in the estimation procedure.

Similar behavior was present for  $b$  values between 0.99 and 1.62. The  $\text{IQR}_{20}/\text{IQR}_6$  ratio also indicates that the scatter in estimated parameters diminishes between 50% and 75% when the sample size goes from 6 to 20 for the three parameters.

Although  $\text{IQR}/X$  does not consider the medium bias, its numerical value gives a good indication of the scatter for the expected value, that is the generator parameter, which is close to the mean value. The  $\text{IQR}/K_{\min}$  and  $\text{IQR}/K_0$  values are very different from each other. When  $n = 30$ ,  $\text{IQR}/K_{\min}$  is approximately 0.6, which means that 50% of the results will be between the median  $\pm 30\%$ , while for  $K_0$  when  $n = 10$ ,  $\text{IQR}/K_0$  is approximately 0.1. This, in turn, means that 50% of the results will be in a range of  $\pm 5\%$  with a significantly lower number of tests. Six tests seem to be sufficient to get a reliable value of  $K_0$ , while the estimations of  $K_{\min}$  are imprecise even for  $n = 30$ .

In the case of  $K_{\min}$ , a still larger scatter was observed for sets with Weibull slope ( $b$ ) greater than 2.

$K_{\min}$  tends to have negative estimated values as the parameter  $b$  increases, which is physically inconsistent, so the software used in the parameter estimation imposes in these cases a value of  $K_{\min} = 0$  (Fig. 3a) [32]. The histogram of  $K_{\min}$  estimations for  $n = 30$  and  $b = 2.99$ , Fig. 3b, shows this effect for all the estimation methods. However, it was smaller when ML was used.

ASTM E1921 methodology was also analyzed, when possible. Figures 6 and 9 ( $K_0$  versus  $n$ ) include the corresponding values of  $\text{IQR}/K_0$  and  $\text{SD}/K_0$ , respectively.

ASTM E1921 requires 6 valid tests to estimate  $K_0$  and then  $T_0$ , and this appears consistent with the results obtained in this paper. However, this does not apply to the other parameters:  $K_{\min}$  and  $b$ , where there is no possibility to have relatively good estimations using sets as large as 30 specimens. According to MCCABE, ZERBST and HEERENS [33], the use of six tests as the minimum number of valid tests to have a good estimation of  $T_0$  is based on a Monte Carlo simulation of the MPC dataset [34, 35] corresponding to 50 1T-CT specimens of an A508 class 3 steel at  $-75^\circ\text{C}$ . MCCABE *et al.* [33] made 100 trials with sets of 3, 4, 5, 6, and 7 specimens, and evaluated the 95% confidence and the standard deviation. They concluded that it appears that six specimen replications make the best compromise result. In the present case, five sets of around 30 specimens from the Euro dataset were analyzed by a rather different methodology as explained above in Sec. 2. For each dataset, the three parameters of the 3P-W distribution were estimated by ML. Then, 3000 datasets of variable

size (from  $n = 5$  to  $n = 60$ ) were generated by the Monte Carlo method and the parameters of the 3P-W distributions that adjust the data were estimated by ML and LR (4 estimators) methods. The goodness of fit was evaluated by IQR and SD. Results confirm with a larger statistical base the requirement of six valid tests to have a good estimation of  $K_0$ .

The results obtained justify the use of two fixed parameters as stated by the standard, not only because of the agreement with experiments but also because it is impractical to obtain the three parameters with an acceptable confidence level.

## 5. CONCLUSIONS

A significant reduction of IQR/X and SD/X values was observed as  $n$  increases. Particularly, this effect is evident for sample sizes between  $n = 6$  and  $n = 20$ . Using  $n = 6$ , IQR/ $K_{\min}$  and IQR/ $b$  showed an important scatter.

$K_0$  parameter can be estimated, with low scatter, by using a relatively small number of specimens, while  $K_{\min}$  and  $b$  need more tests (over 30) for their estimation. No matter whether LR or ML was employed, IQR/X or SD/X tendencies were similar in all cases. The scatter related to  $K_0$  estimated values was at least one order of magnitude smaller than the scatter corresponding to  $K_{\min}$  and  $b$  estimations.

The distribution of  $K_{\min}$  estimated values sometimes showed anomalies, i.e., estimate  $K_{\min}$  as zero, depending on  $b$  values, although this inconsistency starts to vanish for  $b < 2$ . Moreover, this anomaly is lower when using ML. However, ML presented more scatter for estimated values of  $b$ . In addition to this, for some of the analyzed cases, ML showed more dispersion estimating  $K_{\min}$ .

The estimation of  $K_0$  by ASTM presented a similar tendency to the corresponding  $K_0$  value of the 3P-W distribution.

The ASTM E1921 recommendation of two fixed parameters is a good approximation. From a practical point of view, there is no sense trying to estimate accurately  $K_{\min}$  or the parameter  $b$  because, still even if using a quantity of tests as large as 30, result reliability will be very poor. It was verified using more datasets and a larger statistical analysis that six valid tests give a good compromise to estimate  $K_0$ .

## ACKNOWLEDGMENTS

The financial supports of Consejo Nacional de Investigaciones Científicas y Tecnológicas (CONICET) and Consejo de Investigación de la Universidad Nacional de Salta (CIUNSa) are gratefully acknowledged.

## REFERENCES

1. LANDES J.D., SHAFFER D.H., Statistical characterization of fracture in the transition region, [in:] *STP 700 Fracture Mechanics: 12th Conference, West Conshohocken, PA: ASTM International*, Paris P. [Ed.], pp. 368–382, 1980.
2. LANDES J.D., MCCABE D.E., Effect of section size on transition temperature behavior of structural steels, [in:] *STP 833 Fracture Mechanics: 15th Symposium, West Conshohocken, PA: ASTM International*, Sanford R. [Ed.], pp. 378–392, 1984.
3. WALLIN K., SAARIO T., TÖRRÖNEN K., Statistical model for carbide induced brittle fracture in steel, *Metal Science*, **18**(1):13–18, 1984, doi: 10.1179/030634584790420384.
4. WALLIN K., The scatter in  $K_{IC}$ -results, *Engineering Fracture Mechanics*, **19**(6): 1085–1093, 1984, doi: 10.1016/0013-7944(84)90153-X.
5. WALLIN K., Fracture toughness transition curve shape for ferritic structural steels, *Proceedings of International Conference on Fracture of Engineering Materials and Structures*, Singapore, August 6–8, 1991, Teoh S.H., Lee K.H. [Eds.], pp. 83–88, 1991.
6. KIRK M.T., *The technical basis for application of the master curve to the assessment of nuclear reactor pressure vessel integrity*, United States Nuclear Regulatory Commission, ADAMS ML093540004, 2009.
7. WALLIN K., *Fracture Toughness of Engineering Materials: Estimation and Application*, EMAS Publishing, Warrington 2011.
8. ASTM E1921-19b, *Standard Test Method for Determination of Reference Temperature,  $T_0$ , for Ferritic Steels in the Transition Range*, ASTM International, West Conshohocken, PA, 2019, doi: 10.1520/E1921-19B, www.astm.org.
9. HE J., LIAN J., GOLISCH G., JIE X., MÜNSTERMANN S., A generalized Orowan model for cleavage fracture, *Engineering Fracture Mechanics*, **186**: 105–118, 2017, doi: 10.1016/j.engfracmech.2017.09.022.
10. WALLIN K., KARJALAINEN-ROIKONEN P., SUIKKANEN P., Sub-sized CVN specimen conversion methodology, *Procedia Structural Integrity*, **2**: 3735–3742, 2016, doi: 10.1016/j.prostr.2016.06.464.
11. BARBOSA V.S., RUGGIERI C., Fracture toughness testing using non-standard bend specimens – Part II: Experiments and evaluation of  $T_0$  reference temperature for a low alloy structural steel, *Engineering Fracture Mechanics*, **195**: 297–312, 2018, doi: 10.1016/j.engfracmech.2018.03.028.
12. RUGGIERI C., SAVIOLI R.G., DODDS R.H., Comments on W.S. Lei’s discussion of “An engineering methodology for constraint corrections of elastic-plastic fracture toughness – Part II: Effects of specimen geometry and plastic strain on cleavage fracture predictions”, *Engineering Fracture Mechanics*, **178**: 535–540, 2017, doi: 10.1016/j.engfracmech.2016.03.050.
13. BARBOSA V.S., RUGGIERI C., Fracture toughness testing using non-standard bend specimens – Part I: Constraint effects and development of test procedure, *Engineering Fracture Mechanics*, **195**: 279–296, 2018, doi: 10.1016/j.engfracmech.2018.03.029.
14. ISHIHARA K., HAMADA T., MESHII T., T-scaling method for stress distribution scaling under small-scale yielding and its application to the prediction of fracture toughness temperature dependence, *Theoretical and Applied Fracture Mechanics*, **90**: 182–192, 2017, doi: 10.1016/j.tafmec.2017.04.008.

15. MU M.Y., WANG G.Z., XUAN F.Z., TU S.-T., Unified correlation of wide range of in-plane and out-of-plane constraints with cleavage fracture toughness, *Procedia Engineering*, **130**: 803–819, 2015, doi: 10.1016/j.proeng.2015.12.199.
16. MESHII T., Characterization of fracture toughness based on yield stress and successful application to construct a lower-bound fracture toughness master curve, *Engineering Failure Analysis*, **116**: 104713, 2020, doi: 10.1016/j.engfailanal.2020.104713.
17. MESHII T., Failure of the ASTM E 1921 master curve to characterize the fracture toughness temperature dependence of ferritic steel and successful application of the stress distribution T-scaling method, *Theoretical and Applied Fracture Mechanics*, **100**: 354–361, 2019, doi: 10.1016/j.tafmec.2019.01.027.
18. WALLIN K.R.W., Objective assessment of scatter and size effects in the Euro fracture toughness data set, *Procedia Engineering*, **10**: 833–838, 2011, doi: 10.1016/j.proeng.2011.04.137.
19. IPIÑA J.E.P., BEREJNOI C., Size effects in the transition region and the beginning of the upper shelf for ferritic steels, *Fatigue & Fracture of Engineering Materials & Structures*, **33**(3): 195–202, 2010, doi: 10.1111/j.1460-2695.2009.01432.x.
20. LARRAINZAR C., BEREJNOI C., IPIÑA J.E.P., Comparison of 3P-Weibull parameters based on JC and KJC values, *Fatigue & Fracture of Engineering Materials & Structure*, **34**(6): 408–422, 2011, doi: 10.1111/j.1460-2695.2010.01533.x.
21. WEIBULL W., A statistical distribution function of wide applicability, *Journal of Applied Mechanics*, **18**(3): 293–297, 1951, doi: 10.1115/1.4010337.
22. PRABHAKAR MURTHY D.N., XIE M., JIANG R., *Weibull Models*, John Wiley & Sons, Hoboken, New Jersey, 2004.
23. DODSON B., *The Weibull Analysis Handbook*, ASQ Quality Press, 2006.
24. SANDON F., “Mathematics of Statistics. II” by J.F. Kenney. Pp. ix, 202. 15s. 1939; rep. 1947 (Van Nostrand, New York; Macmillan, London), *The Mathematical Gazette*, **33**(305): 228–229, 1949, doi: 10.2307/3611432.
25. HEERENS J., HELLMANN D., Development of the Euro fracture toughness dataset, *Engineering Fracture Mechanics*, **69** (4): 421–449, 2002, doi: 10.1016/S0013-7944(01)00067-4.
26. KNUTH D.E., *The Art of Computer Programming, Vol. 2. Seminumerical Algorithms* (3rd ed.), Addison-Wesley Longman Publishing Co., Inc., 1997.
27. POBOČÍKOVÁ I., SEDLIAČKOVÁ Z., Comparison of four methods for estimating the Weibull distribution parameters, *Applied Mathematical Sciences*, **8**(83): 4137–4149, 2014, doi: 10.12988/ams.2014.45389.
28. FERREIRA L.A., SILVA J.L., Parameter estimation for Weibull distribution with right censored data using EM algorithm, *Eksploatacja i Niezawodność – Maintenance and Reliability*, **19**(2): 310–315, 2017, doi: 10.17531/ein.2017.2.20.
29. NG H.K.T., LUO L., HU Y., DUAN F., Parameter estimation of three-parameter Weibull distribution based on progressively Type-II censored samples, *Journal of Statistical Computation and Simulation*, **82**(11): 1661–1678, 2012, doi: 10.1080/00949655.2011.591797.
30. KENNEY J.F., *Mathematics of Statistics*, Chapman & Hall LTD, London, 1947.
31. WALLIN K., Master curve Analysis of the “Euro” fracture toughness dataset, *Engineering Fracture Mechanics*, **69**(4), 451–481, 2002, doi: 10.1016/S0013-7944(01)00071-6.

32. IPIÑA J.E.P., CENTURION S.M.C., ASTA E.P., Minimum number of specimens to characterize fracture toughness in the ductile-to-brittle transition region, *Engineering Fracture Mechanics*, **47**(3): 457–463, 1994, doi: 10.1016/0013-7944(94)90102-3.
33. McCABE D.E., ZERBST U., HEERENS J., *Development of Test Practice Requirements for a Standard Method on Fracture Toughness Testing in the Transition Regime* (Report GKSS–93/E/81), Germany, 1993.
34. MIGLIN M., OBERJOHN L., VAN DER SLUYS W., Analysis of results from the MPC/JSPS round robin testing program in the ductile-to-brittle transition region, [in:] *Fracture Mechanics: Twenty-Fourth Volume*, J. Landes, D. McCabe, J. Boulet [Eds], West Conshohocken, PA: ASTM International, pp. 342–354, 1994, doi: 10.1520/stp13713s.
35. VAN DER SLUYS W., MIGLIN M., Results of MPC/JSPS cooperative testing program in the brittle-to-ductile transition region, [in:] *Fracture Mechanics: Twenty-Fourth Volume*, J. Landes, D. McCabe, J. Boulet [Eds], West Conshohocken, PA: ASTM International, pp. 308–324, 1994, doi: 10.1520/STP13711S.

*Received April 15, 2020; accepted version February 11, 2021.*

---

*Published on Creative Common licence CC BY-SA 4.0*

